ELSEVIER

Journal of Wind Engineering
and Industrial Aerodynamics 94 (2006) 859–881

JOURNAL OF wind engineering AND industrial aerodynamics

www.elsevier.com/locate/jweia

Application of indicial functions in bridge deck aeroelasticity

Carlotta Costa, Claudio Borri*

Dipartimento di Ing. Civile, Università di Firenze, Via di S. Marta 3, 50142 Firenze, Italy

Available online 25 September 2006

Abstract

This contribution deals with some recent studies on numerical and analytical models for the evaluation of aeroelastic response of cross-section models of long span bridges. The time-domain indicial approach, whose validity has been only partially investigated in the past, is selected for the modeling of self-excited forces. Sets of indicial function coefficients are estimated for rectangular cross-sections, and their applicability is proven, through time-domain simulations and comparison with experimental tests. Critical flutter condition and dynamic pre-critical and post-critical behaviors are evaluated.

Keywords: Bridge aeroelasticity; Time-domain simulations; Unsteady forces; Indicial functions; Flutter instability

1. Introduction

A gradual and constant increase in span length, as well as a constant research of lightness and attractiveness, can be recognized in modern bridge and footbridge design. Well-known examples are, among the others, the Great Belt East Bridge (Denmark, 1998, 1624 m), the design of Messina Strait Crossing (Italy, 3300 m), the Millennium footbridge (London, Great Britain, 332 m). In the other hand, such structures are often characterized by high flexibility and sensitivity to wind action, which can give rise to local or global instability phenomena compromising serviceability or even structural safety. Among these phenomena, vortex shedding, buffeting and flutter may play an important role.

*Corresponding author.
E-mail address: cborri@dicea.unifi.it (C. Borri).

0167-6105/$ - see front matter
doi:10.1016/j.jweia.2006.06.007

In the modeling of wind action on structures, different contributions trying to capture such different aspects are identified: (i) a steady component, depending on mean wind velocity; (ii) a buffeting component depending on turbulent wind fraction , (iii) a vortex-shedding component, due to synchronized flow separation and (iv) a self-excited component depending on structural motion. Usually, these aspects are considered separately. It is assumed, in fact, that they are related to different wind and frequency ranges and, therefore, their interaction is negligible. This is, in principle, not true, but such a scheme has proven to be satisfying for the description of several phenomena. In this work, attention is focused on flutter instability, which is assumed totally dependent on self-excited forces. Different types of flutter instabilities can be identified depending on flow distribution and structural geometry, as described in detail by Matsumoto et al. (2002). In every case, structural damping and stiffness, as well as natural frequencies, are altered by aerodynamic terms due to wind action. Different incoming wind speeds, therefore, modify structural behavior, and also could drive the structure to failure. Then, the identification of the flutter mechanism and of the conditions under which it can occur represents a fundamental step in bridge and footbridge design.

Traditional approaches for the analysis are in frequency and time domain. The spectral approach is adopted to capture the main features of the dynamic problem. Thus, nonlinear and nonstationary features, as well as evolution of dynamic properties with varying ambient loadings, can be taken into account only with time-domain analyses. Without reliable estimations of such behavior, satisfactory performance of structures cannot be assured and the state-of-the-art in structural design cannot advance. In the other hand, simulations in time domain are only a quite recent achievement, requiring appropriate numerical tools to obtain accurate results with a reasonable computational cost.

In this paper, the behavior of rectangular cross-sections under self-excited forces is considered, for a wide range of incoming mean wind velocities. Attention is focused on time-domain modeling. Among time-domain approaches, the indicial one is selected. Indicial theory is noteworthy in aeronautical field, while his extension to bridge engineering represents a quite recent challenge. Its application, in fact, needs to be properly calibrated and discussed.

1.1. Background

Load models commonly used to pattern wind action on bridges follow the work of Scanlan and Tomko (1971). As a matter of fact, no theoretical formulation is available to treat aeroelastic problems for bluff bodies like bridges. The main hypotheses on which thin airfoil theory is based, as existence of potential flow, no separation of shear layers and full gust coherence, do not apply strictly to bodies with different geometrical shapes. Therefore, the formulation of the external loads follows the guidelines of aerodynamic theory, but needs to adapt itself to the special case of each bridge, by means of suitable experimental data. The approach suggested by Scanlan and co-workers is linear and superimposes buffeting forces due to turbulent wind components and self-excited forces due to flow–structure interaction. Both buffeting and self-excited forces are included in a time–domain framework, common also to thin airfoil aerodynamics, and characterized by frequency-dependent functions. Self-excited forces, in particular, are modeled by means of *aeroelastic* or *flutter derivatives*. These frequency-dependent functions are generally

available as discrete-frequency parameters measured in wind tunnel tests by Simiu and Scanlan (1986).

The analogous quantities, valid for a thin airfoil, can be defined in terms of *Theodorsen's circulation* function Theodorsen (1935), which describes the evolution of self-excited lift on an airfoil in sinusoidal motion.

A representation of self-excited actions completely in time domain, without explicit dependence on frequency, can be provided, if appropriate functions are defined. Such functions describe, according to thin airfoil theory, time development of sectional forces due to structural motions. If arbitrary motions are considered, total action can be calculated via convolution. In thin airfoil theory, *Wagner's* function Wagner (1925) provides self-excited lift and moment due to an elementary step change in the angle of attack, that is in the relative placement of the section with respect to the incident flow. Such function is usually referred to as an *indicial* function.

Corresponding indicial functions for bridges can be defined in a similar manner, as *Wagner-like* functions, and can be calculated from aeroelastic derivatives or directly identified in wind tunnel tests.

1.2. Literature survey: indicial functions to model self-excited loads

As already recalled, the first indicial function is considered to be the Wagner's function, analytically defined for lift on a thin airfoil (referred to also as an ideal *flat plate*). A common approximation of Wagner's function is due to Jones (1940), as the sum of exponential functions, suitable for Fourier-transforming. More general functions are proposed by Bisplinghoff et al. (1955), for describing aerodynamic moment and distinguishing the effects of the different components of the motion on self-excited loads.

For bridges, thus, the first relevant work suggesting the possibility of using indicial functions is due to Scanlan et al. (1974). The expression of indicial functions is based on the exponential approximation of Wagner's function. Equivalence with mixed time-frequency models is suggested, examples of indicial functions for various bridge decks are provided, and relationships between indicial function coefficients and aeroelastic derivatives are stated.

This formulation of self-excited forces is obtained directly in analogy with aerodynamic formulation, and adapted to the more general case of bluff sections. This model of self-excited forces will be called, here, *Scanlan's formulation*.

Lin and Ariaratnam (1980) and Lin and Li (1993) consider a model with the sole torsional degree of freedom (DoF), to capture the torsional flutter typical of bluff bodies. The attention is focused on stochastic effects induced by turbulence. The expression of self-excited forces proposed in such works is slightly different from the one derived by Scanlan and co-workers, directly obtained from thin airfoil theory. It will be referred, in this context, as *Lin's formulation*. The adoption of such formulation is justified as the most suitable for stochastic analyses.

An analogous formulation of self-excited forces is used by Borri and Höffer (2000) and by Borri et al. (2002), to reproduce both torsional and coupled flutter. In fact, translational DoFs and corresponding self-excited forces are included. Moreover, the computational efficiency of the indicial scheme is afforded, by proposing an incremental form suitable for numerical implementation. Borri and Höffer (2000) suggest the possibility of modeling the fading memory of self-excited forces, as the fluid enveloping the body interacts with the

body in motion. The fading memory is included in a finite element code by Borri et al. (2002). First analyses on the memory effects of self-excited forces on the effective evolution of bridge motion are carried out. Sectional forces are taken into account, neglecting the effective three-dimensional behavior of the bridge, i.e. the possibility of lateral motion and relevant vibration modes and self-excited forces.

A crucial step in indicial modeling is the identification of indicial function coefficients. The calibration of such parameters is usually performed via a minimization of an error vector, in order to fit experimental data. A nonlinear least-square procedure is proposed by Scanlan et al. (1974). A scheme, based on the Levenberg–Marquardt method, is adopted by Caracoglia and Jones (2003a, b), and applied to different bridge deck cross-sections, considering the Scanlan's formulation of self-excited forces. Zahlten et al. (2004) highlight main advantages and difficulties of various iterative methods to solve identification problem, with particular attention on the specific case of indicial parameters, adopting Lin's formulation. Strongly different sets of indicial functions, all well approximating aeroelastic derivatives, lead to analogous estimation of the critical flutter condition. The values of coefficients are, therefore, clearly dependent on the formulation of the load model, which is of relevant significance.

By following the operational treatment of Roger (1977), aeroelastic derivatives functions can be approximated, in the Laplace domain, by means of a series of rational functions independent of frequency. For bridges, such an approach is adopted by Bucher and Lin (1989), in a stochastic analysis to define the effect of turbulence on flutter threshold and by Wilde et al. (1996), in a state-space formulation suitable for passive and active control for flutter. Among the others, Boonyapinyo et al. (1999) and Chen et al. (2000) use rational function approximation in the context of a finite element approach, to simulate the motion of a full bridge in turbulent flow. Substantial equivalence between formulations with rational and indicial functions can be demonstrated Lazzari et al. (2004). Filters of high order are, usually, required to approximate aeroelastic derivatives with rational functions, while indicial functions retain the advantage of being interpretable as physically meaningful quantities and, in most cases, require a smaller number of parameters, as it will be demonstrated in this paper.

First experimental attempts for bridge deck sections are due to Caracoglia and Jones (2003a, b) and Zhang et al. (2003), but a sufficient standardization of the procedures is still not achieved.

Rectangular cross-sections are considered here. References to the aeroelastic behavior of such cross-sections are furnished, for example, by Matsumoto et al. (1996).

1.3. Issues addressed in this paper

In this paper, indicial approach for self-excited forces is thoroughly analyzed. In particular, a load scheme following Scanlan's formulation is build up and sets of indicial coefficients are obtained for a 'streamlined' and a 'bluff' rectangular section.

Insights on different formulations of indicial function load models for self-excited forces are given, in order to justify the adoption of such formulation.

The feasibility of the selected approach is demonstrated, at least in the case of cross-sectional analyses, by the identification of critical flutter condition, pre-critical and post-critical behavior. Comparisons amongst wind tunnel tests, numerical and analytical procedures are carried out. No direct comparison, involving time-domain simulations of

cross-sectional response and experimental tests, has been found in literature, neither analyses on the effect of different group of coefficients on the dynamic behavior of the section.

It is shown that, in the case of streamlined section, aeroelastic behavior can be represented with sufficiently good approximation with only one exponential group, while more 'bluff' geometries require an augmented number of states. In the 'bluff' case, a limited number of indicial coefficients does not represent in an adequate manner the unsteady contribution of self-excited forces. Coupled and torsional flutter conditions are well captured by numerical simulation.

2. Mechanical system

The mechanical system is a rectangular symmetric cross-section simulating an elementary strip of a bridge deck (Fig. 1). The main characteristic dimension is assumed to be the width of the deck section B, referred to as the *chord*. The *half-chord* is indicated with $b = B/2$. The thickness of the section is indicated with D, the span of the bridge with L.

The dimensional ratio B/D between chord and thickness is a common parameter to describe the slenderness of the structure, i.e. the optimization in the aerodynamic sense. Even if a rectangular section shows separation of flow in correspondence of sharp edges, for a section sufficiently elongated, flow reattaches and aerodynamic behavior is similar to that one of an ideal flat plate. An 'optimized' section is referred to also as *streamlined*, in contrast with a *bluff* section, in which separation of shear layers strongly affects the vortex street. Quasi-steady theory can qualitatively describe dynamic behavior of streamlined sections, while unsteady effects become fundamental for bluff sections.

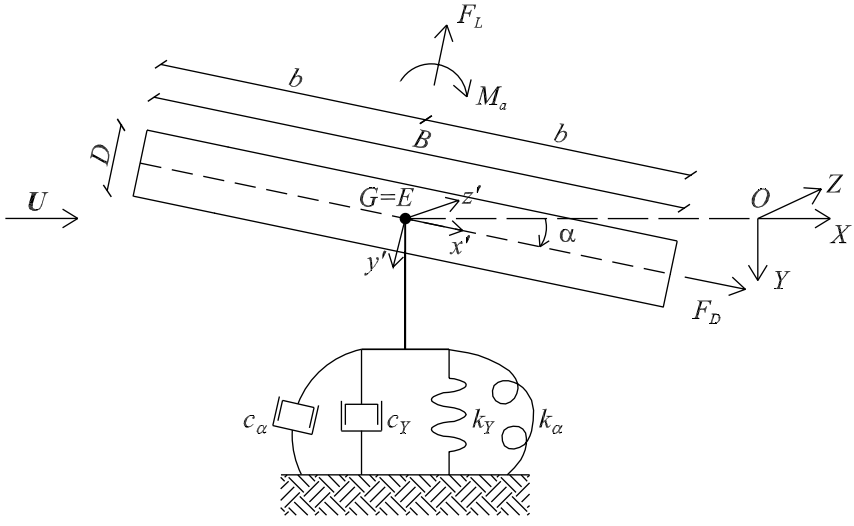

Fig. 1. Mechanical scheme (B = chord; b = half-chord; D = thickness; k_Y = translational stiffness; k_α = rotational stiffness; c_Y = translational damping; c_α = rotational damping), relevant points (G = center of mass; E = elastic center), wind forces (F_L = lift force; F_D = drag force; M_a = aerodynamic moment), wind flow (U = wind velocity), global reference system ($OXYZ$) and local reference system ($Gx'y'z'$).

The system is supposed to exhibit only vertical DoF y (*heaving*) and rotational DoF α (*torsion*). Horizontal displacements are neglected. The cross-section is studied, at this stage, as a rigid body, with mass properties concentrated in the center of mass G. Elastic properties are resumed by springs of stiffness k_y and k_α, damping properties by c_y and c_α damping coefficients. The elastic center E corresponds to the application point of dampers and springs, and, in force of the assumed symmetry of the section, is coincident with the center of mass G. They are both located at the midspan of the section.

Two reference frames are defined: a first Cartesian inertial reference frame $OXYZ$ and a second coordinate system $Gx'y'z'$, joint to the vibrating structure, with the origin coincident with center of mass G and x' and y' axes oriented, respectively, along the sectional middle line chord and the orthogonal direction.

The reference frames are assigned following '*airfoil convention*', namely positive vertical translations are directed downwards and positive rotations are clockwise.

The equations of motion describing the dynamic system, per unit length, are given by

$$\begin{aligned} &m\ddot{y} + c_y\dot{y} + k_y y = F_Y, \\ &I\ddot{\alpha} + c_\alpha\dot{\alpha} + k_\alpha\alpha = M_Z, \end{aligned} \tag{1}$$

where m is mass and I mass momentum of inertia.

Resulting wind force acting on the section are decomposed as the combination of a lift force F_L, a drag force F_D and an aerodynamic moment M_a, applied on the center of mass G. Lift and drag force act, respectively, along the y' and the x' axes. Aerodynamic moment acts about the $z' \equiv Z$-axis directed along the bridge span, namely $M_a \equiv M_Z$. Vertical force F_Y is obtained combining lift and drag forces with reference to the global coordinate system:

$$F_Y = -F_L \cos\alpha + F_D \sin\alpha. \tag{2}$$

'*Airfoil convention*' is adopted also in wind load representation, that is lift force F_L is positive upwards and aerodynamic moment M_a is positive clockwise.

Linearized theory is adopted, that is the *angle of attack* α—defined as the angle between the section chord and the main flow direction–is small. This allows one to assume that $|F_Y| = |F_L|$.

3. Wind field

The section is immersed in a wind field, assumed incompressible and non-viscous. The wind velocity U_w can be decomposed additively as a time–space variable field

$$U_w(M,t) = U(M) + U'(M,t), \tag{3}$$

where t is the time, U the mean wind speed and U' represents a turbulent perturbation, acting at point M of coordinates X_M, Y_M and Z_M.

Mean wind is directed along the X-axis, while the turbulence field, in this simplified case, has not significant components. Therefore, the flow is smooth and the resultant wind field is given by

$$U_{wX}(M,t) = U(M), \quad U_{wY}(M,t) = 0, \quad U_{wZ}(M,t) = 0. \tag{4}$$

4. Time-dependent sectional forces

Sectional time-varying wind load can be expressed, by assuming validity of superposition principle and neglecting vortex-shedding and buffeting contributions, as

$$F_{\mathrm{L}}(t) = F_{\mathrm{Lse}}(t), \quad M_{\mathrm{a}}(t) = M_{\mathrm{ase}}(t), \tag{5}$$

where subscript se indicates self-excited forces.

In this case, dead loads and static wind forces are neglected.

4.1. Self-excited forces

The most common expression for sectional self-excited forces, in the mixed time-frequency domain, is, considering a sinusoidal coupled motion of reduced frequency $K = \omega B/U$ Scanlan and Jones (1990),

$$\begin{aligned} F_L(t) &= qB\left[KH_1^*(K)\frac{\dot{y}(t)}{U} + KH_2^*(K)\frac{B\dot{\alpha}(t)}{U} + K^2H_3^*(K)\alpha(t) + K^2H_4^*(K)\frac{y(t)}{U}\right], \\ M_a(t) &= qB^2\left[KA_1^*(K)\frac{\dot{y}(t)}{U} + KA_2^*(K)\frac{B\dot{\alpha}(t)}{U} + K^2A_3^*(K)\alpha(t) + K^2A_4^*(K)\frac{y(t)}{U}\right], \end{aligned} \tag{6}$$

where ρ is the air density, $q = 1/2\rho U^2$ is the the kinetic pressure, and H_i^* and $A_i^*(i = 1,\ldots,4)$ are the aeroelastic derivatives, commonly identified in wind tunnel tests as function of reduced frequency K or reduced velocity $U_{\mathrm{red}} = 2\pi/K = 2\pi U/\omega B$.

In the pure time-domain framework, self-excited forces are defined by means of *indicial* functions, alternatively as a function of t or dimensionless time $s = Ut/b$, as common in wing aerodynamics. Following the scheme of wing theory Fung (1969), lift force and moment can be defined, adopting Scanlan's formulation, as follows:

$$\begin{aligned} F_{\mathrm{L}}(s) &= qB\frac{\mathrm{d}C_L}{\mathrm{d}\alpha}\left[\frac{2}{B}y'(0)\Phi_{Ly}(s) + \alpha(0)\Phi_{L\alpha}(s)\right. \\ &\quad \left. + \int_0^s \Phi_{Ly}(s-\sigma)\frac{2}{B}y''(\sigma)\,\mathrm{d}\sigma + \int_0^s \Phi_{L\alpha}(s-\sigma)\alpha'(\sigma)\,\mathrm{d}\sigma\right], \\ M_{\mathrm{a}}(s) &= q\frac{B^2}{U}\frac{\mathrm{d}C_M}{\mathrm{d}\alpha}\left[\frac{2}{B}y'(0)\Phi_{My}(s) + \alpha(0)\Phi_{M\alpha}(s)\right. \\ &\quad \left. + \int_0^s \Phi_{My}(s-\sigma)\frac{2}{B}y''(\sigma)\,\mathrm{d}\sigma + \int_0^s \Phi_{M\alpha}(s-\sigma)\alpha'(\sigma)\,\mathrm{d}\sigma\right], \end{aligned} \tag{7}$$

where $\Phi_{hk}(s)$ are the indicial functions ($h = L, M$; $k = y, \alpha$). Prime denotes differentiation with respect to s, dot with respect to t. Derivatives of aerodynamic coefficients $\mathrm{d}C_h/\mathrm{d}\alpha$ are calculated with respect to steady angle of attack.

Scanlan's formulation of Eq. (7) is obtained directly in analogy with wing theory. Wing theory uses only one indicial function, that is the Wagner's function, to describe the evolution of self-excited forces due to elementary step changes in configuration. Following this idea and considering Eq. (7), each indicial function describes the evolution of a self-excited force component due to an elementary step change in configuration. Sectional configuration is completely defined by angle of attack, which is expressed by means of incoming wind speed, vertical velocity, torsional displacement and velocity of the section

(see Fung, 1969). In the case of thin airfoil, contributions due to vertical velocity, torsional displacement and torsional velocity are identically treated. This is not valid in the case of bluff bodies, because different indicial functions are required, in principle, to describe responses to step changes in vertical velocity, torsional displacement and torsional velocity. Moreover, without loss of generality, for a bluff body, angle of attack can be expressed by torsional displacement and vertical velocity, without including explicitly the effect of torsional velocity. This assumption has been firstly suggested by Bucher and Lin (1989) and is retained in this work. Therefore, for each self-excited force component, only two indicial functions are required to define the total force.

Indicial functions are here defined as the superposition of a constant part a_{0hk}, accounting for quasi-steady effects, and n exponential groups characterized by the pairs of coefficients (a_{ihk}, b_{ihk}), describing the unsteady evolution of the force:

$$\Phi_{hk}(s) = a_{0hk} - \sum_{i=1}^{n} a_{ihk} \exp(-b_{ihk} s). \tag{8}$$

Each coefficient is identified by three indices: the first (i) is the sum index, the second (L or M) establishes the aeroelastic component of interest, while the third defines the varying displacement (α) or velocity (y').

4.1.1. A suitable formulation for numerical procedures

The integro-differential problem of Eq. (7) can be adjusted in order to calculate the response, by performing a simple integration by parts. The following scheme is obtained, suitable of numerical implementation:

$$\begin{aligned}
F_{\mathrm{L}}(s) &= qB\frac{\mathrm{d}C_{\mathrm{L}}}{\mathrm{d}\alpha}\left[\Phi_{Ly}(0)\frac{2}{B}y'(s) + \Phi_{L\alpha}(0)\alpha(s)\right.\\
&\quad \left. + \int_0^s \Phi'_{Ly}(s-\sigma)\frac{2}{B}y'(\sigma)\,\mathrm{d}\sigma + \int_0^s \Phi'_{L\alpha}(s-\sigma)\alpha(\sigma)\,\mathrm{d}\sigma\right],\\
M_{\mathrm{a}}(s) &= q\frac{B^2}{U}\frac{\mathrm{d}C_M}{\mathrm{d}\alpha}\left[\Phi_{My}(0)\frac{2}{B}y'(s) + \Phi_{M\alpha}(0)\alpha(s)\right.\\
&\quad \left. + \int_0^s \Phi'_{My}(s-\sigma)\frac{2}{B}y'(\sigma)\mathrm{d}\sigma + \int_0^s \Phi'_{M\alpha}(s-\sigma)\alpha(\sigma)\,\mathrm{d}\sigma\right].
\end{aligned} \tag{9}$$

An analogous time domain formulation can be provided, accounting for indicial functions with time dependency:

$$\begin{aligned}
F_{\mathrm{L}}(t) &= qB\frac{\mathrm{d}C_L}{\mathrm{d}\alpha}\left[\hat{\Phi}_{Ly}(0)\frac{2}{B}\dot{y}(t) + \hat{\Phi}_{L\alpha}(0)\alpha(t)\right.\\
&\quad \left. + \int_0^t \dot{\hat{\Phi}}_{Ly}(t-\sigma)\frac{2}{B}\dot{y}(\sigma)\,\mathrm{d}\sigma + \int_0^t \dot{\hat{\Phi}}_{L\alpha}(t-\sigma)\alpha(\sigma)\,\mathrm{d}\sigma\right],\\
M_a(t) &= q\frac{B^2}{U}\frac{\mathrm{d}C_M}{\mathrm{d}\alpha}\left[\hat{\Phi}_{My}(0)\frac{2}{B}\dot{y}(t) + \hat{\Phi}_{M\alpha}(0)\alpha(t)\right.\\
&\quad \left. + \int_0^t \dot{\hat{\Phi}}_{My}(t-\sigma)\frac{2}{B}\dot{y}(\sigma)\,\mathrm{d}\sigma + \int_0^t \dot{\hat{\Phi}}_{M\alpha}(t-\sigma)\alpha(\sigma)\,\mathrm{d}\sigma\right],
\end{aligned} \tag{10}$$

where $\hat{\Phi}_{hk}(t)$ are the indicial functions ($h = L, M$; $k = y, \alpha$), defined as

$$\hat{\Phi}_{hk}(t) = a_{0hk} - \sum_{i=1}^{n} a_{ihk} \exp\left(-b_{ihk} \frac{2U}{B} t\right). \tag{11}$$

4.1.2. A suitable formulation for numerical procedures

If dimensionless time formulation of Eq. (9) is adopted, in order to keep the direct relationship with wing theory, following equivalence scheme between aeroelastic derivatives and indicial function coefficients holds true:

$$\begin{aligned}
\frac{2\pi}{U_{\text{red}}} H_1^* &= \frac{\mathrm{d}C_L}{\mathrm{d}\alpha}\left[1 - \sum_i a_{iLy} \frac{\pi^2}{b_{iLy}^2 U_{\text{red}}^2 + \pi^2}\right],\\
\frac{2}{U_{\text{red}}^2} H_4^* &= \frac{\mathrm{d}C_L}{\mathrm{d}\alpha}\left[\sum_i a_{iLy} \frac{b_{iLy}}{b_{iLy}^2 U_{\text{red}}^2 + \pi^2}\right],\\
\frac{4\pi}{U_{\text{red}}^3} H_2^* &= \frac{\mathrm{d}C_L}{\mathrm{d}\alpha}\left[\sum_i -a_{iL\alpha} \frac{b_{iL\alpha}}{b_{iL\alpha}^2 U_{\text{red}}^2 + \pi^2}\right],\\
\frac{4\pi^2}{U_{\text{red}}^2} H_3^* &= \frac{\mathrm{d}C_L}{\mathrm{d}\alpha}\left[1 - \sum_i a_{iL\alpha} \frac{\pi^2}{b_{iL\alpha}^2 U_{\text{red}}^2 + \pi^2}\right],
\end{aligned} \tag{12}$$

$$\begin{aligned}
\frac{2\pi}{U_{\text{red}}} A_1^* &= \frac{\mathrm{d}C_M}{\mathrm{d}\alpha}\left[1 - \sum_i a_{iMy} \frac{\pi^2}{b_{iMy}^2 U_{red}^2 + \pi^2}\right]\\
\frac{2}{U_{\text{red}}^2} A_4^* &= \frac{\mathrm{d}C_M}{\mathrm{d}\alpha}\left[\sum_i a_{iMy} \frac{b_{iMy}}{b_{iMy}^2 U_{\text{red}}^2 + \pi^2}\right],\\
\frac{4\pi}{U_{\text{red}}^3} A_2^* &= \frac{\mathrm{d}C_M}{\mathrm{d}\alpha}\left[\sum_i -a_{iM\alpha} \frac{a_{iM\alpha}}{b_{iM\alpha}^2 U_{\text{red}}^2 + \pi^2}\right],\\
\frac{4\pi^2}{U_{\text{red}}^2} A_3^* &= \frac{\mathrm{d}C_M}{\mathrm{d}\alpha}\left[1 - \sum_i a_{iM\alpha} \frac{\pi^2}{b_{iM\alpha}^2 U_{\text{red}}^2 + \pi^2}\right].
\end{aligned} \tag{13}$$

Derivatives of aerodynamic coefficients with respect to the angle of attack (sometimes referred to as *dynamic derivatives*) appear, to account for the limit case of quasi-steady behavior, corresponding to very low frequencies. These coefficients are, in principle, different from those of thin airfoil, which are $\mathrm{d}C_L/\mathrm{d}\alpha = 2\pi$ and $\mathrm{d}C_M/\mathrm{d}\alpha = \pi/4$.

A nonlinear least-square method is applied to identify indicial function coefficients from aeroelastic derivatives, following the equivalence scheme of Eqs. (12) and (13). Once a prescribed number i of exponential groups characterizing each indicial function is fixed, and experimental aeroelastic derivatives are assigned, an appropriate function identifies the values of coefficients $\mathbf{a}_{ihk}$, $\mathbf{b}_{ihk}$ and $\mathrm{d}C_h/\mathrm{d}\alpha$ which minimize the norm E, defined as

$$E = \sum_{j=1}^{4} \left\| \mathbf{H}_j^* - \mathbf{H}_j^*(\text{exp.}) \right\|, \tag{14}$$

where $\mathbf{H}_j^*$(exp.) are the experimental aeroelastic derivatives, while $\mathbf{H}_j^*$ are the calculated estimates. The most general choice of parameters includes indicial coefficients and derivatives of aerodynamic coefficients, with the simultaneous optimization on four derivatives. Aerodynamic coefficients and its derivatives can also be measured and, therefore, treated as known values. By this way, the error estimation would be performed only on two derivatives at a time, with a great reduction of optimization parameters.

4.1.3. Lin's formulation

In this section, Lin's formulation Lin and Ariaratnam (1980) is recalled, and extended in order to include lift force Borri and Höffer (2000):

$$\begin{aligned} F_{\mathrm{L}}(t) &= qB\frac{\mathrm{d}C_L}{\mathrm{d}\alpha}\left[\mathrm{d}_{Ly}\frac{\dot{y}(t)}{U}+d_{L\alpha}\frac{B\dot{\alpha}(t)}{U}\right.\\ &\quad\left.+\int_{-\infty}^{t}\varphi_{Ly}(t-\sigma)\frac{\dot{y}(\sigma)}{B}\,\mathrm{d}\sigma+\int_{0}^{t}\varphi_{L\alpha}(t-\sigma)\dot{\alpha}(\sigma)\,\mathrm{d}\sigma\right]\\ M_{\mathrm{a}}(t) &= q\frac{B^2}{U}\frac{\mathrm{d}C_M}{\mathrm{d}\alpha}\left[d_{My}\frac{\dot{y}(t)}{U}+d_{M\alpha}\frac{B\dot{\alpha}(t)}{U},\right.\\ &\quad\left.+\int_{0}^{t}\varphi_{My}(t-\sigma)\frac{\dot{y}(\sigma)}{B}\mathrm{d}\sigma+\int_{0}^{t}\varphi_{M\alpha}(t-\sigma)\alpha(\sigma)\,\mathrm{d}\sigma\right], \end{aligned} \tag{15}$$

where indicial functions are indicated with φ_{ij} ($i = L, M$; $j = y, \alpha$) and different coefficients do appear, namely d_{hk}, as quasi-steady terms with unclear relationships with indicial functions. Moreover, effects of torsional motion on self-excited loads are taken into account by means of torsional velocity, rather than through angle of attack.

In this paper, the Scanlan-like formulations of Eqs. (9) and (10) are adopted, because no additional constants are needed, and the identification can be more easily performed. Moreover, the number of parameters required adopting such formulation is already sufficient to reproduce sectional behavior.

5. Numerical analyses

As already observed, the system of integro-differential equations modeling the mechanical system includes memory effects, in the sense that the state of the system and the way in which it evolves in time are dependent upon actual and past states. Equations that include convolution terms are the classical Volterra integral equation of the second kind.

Attention must be paid to the choice of the algorithm, because the necessary accuracy, stability and preservation of qualitative behavior must be guaranteed. In particular, a high numerical sensitivity of the system is evidenced in the numerical solution. Time steps need to be small, to evaluate correctly convolution terms and response.

A fourth-order Runge–Kutta (RK) algorithm is adapted to this case, in order to include the fading memory of self-excited forces. Equations of motion including self-excited forces as described in Eq. (10) are reduced to a first-order differential problem. The evaluation of the convolution integral is performed by means of rectangular rule, by taking into account all the displacement and velocity histories of the section, since the time origin. The whole history motion has to be stored and used to evaluate the convolutions, therefore

computational effort increases rapidly with the simulation length. In this sense, it can be useful to account for fading memory to reduce the computational effort, as proposed by Borri and Höffer (2000) and applied by Borri et al. (2002), considering a moving time window that includes only the last part of the unsteady forces. In fact, the unsteady contribution of each elementary force tends to a quasi-steady value, and, therefore, its effect on the actual time decreases, as integration time increases.

If this fourth-order RK algorithm is compared with Newmark-β type algorithms, it can be observed that conditionally stable Newmark-β ($\alpha = 1/2$, $\delta = 1/6$) achieves results with comparable accuracy, while a Newmark-β algorithm unconditionally stable ($\alpha = 1/2$, $\delta = 1/4$) requires time steps ten times smaller. For large analyses, as, in perspective, those ones involving finite-element analyses and full bridges, RK methods become too time-consuming, at least in the formulation adopted here, and Newmark-β procedures can represent a good alternative.

5.1. A 'streamlined' section

A rectangular section, with features given in Table 1, is analyzed. Dimensional ratio is $B/D = 12.5$.

Critical flutter condition, as well as dynamic behavior in pre-critical and post-critical ranges, are calculated and compared, by means of estimation of indicial coefficients and numerical simulations. In particular, flutter velocity and frequency are identified, both through classical eigenvalue analysis Dyrbye and Hansen (1996) and numerical simulations performed with indicial function coefficients obtained from experimental data.

5.1.1. Identification of indicial function coefficients

In the following, aeroelastic derivatives are taken according to Matsumoto et al. (1996). Discrete data are interpolated by means of polynomial functions, with a third-order polynomial approximation for all aeroelastic derivatives and a second order approximation chosen for A_2^*. It is worth to recall that a strong influence of the interpolating functions can be observed both on eigenvalue analysis and indicial coefficient identifications, and, therefore, on numerical simulations. Attention must be paid to the original experimental data and to their consistency.

The simplest form is inferred to all indicial functions, with only one exponential group, i.e. $\Phi_{hk}(s) = 1 - a_{1hk} \exp(-b_{1hk})$.

In fact, this section has an 'aerodynamic' behavior, by comparison of experimental and theoretical aeroelastic derivatives calculated on the basis of Theodorsen's circulation function, i.e. with flat plate theoretical values. In thin airfoil, the unique Wagner's

Table 1
Geometrical and mechanical properties—rectangular section $B/D = 12.5$

L (m)	b (m)	ω_y (rads^{-1})	f_Y (Hz)	m (kg/m)	ζ_y (−)
0.920	0.1875	36.88	5.87	3.810	0.0018
D (m)	B (m)	ω_α (rad^{-1})	f_α (Hz)	I (kg/m)	ζ_α (−)
0.03	0.375	52.15	8.30	0.037	0.0028

function, in the approximation with two exponential groups, well describes lift force and moment. Therefore, for a 'streamlined' section as $B/D = 12.5$, it is expected that two functions characterized by one exponential group should be sufficient to capture main dynamic features. Aerodynamic coefficients are treated as unknown quantities, therefore estimated simultaneously with indicial coefficients.

The values obtained for aerodynamic coefficients loose the proper physical meaning, becoming, more properly, scale parameters, strongly dependent on the input data.

The approximations of aeroelastic derivatives via indicial functions are plotted in Figs. 2 and 3. In particular, a satisfying approximation is achieved for all lift and moment flutter derivatives H_i^* (exp.) and A_i^* (exp.) (for $i = 1,\ldots,4$), with indicial functions characterized by parameters of Table 2 and dynamic derivatives of Table 3.

5.1.2. *Numerical simulations under wind loading*

Sectional behavior is evaluated in various ranges of incoming wind. The fourth-order RK algorithm is adopted, with a selected time step $\Delta t = 0.001$ s.

As examples, vertical and torsional histories, as well as power spectral density functions, are directly compared with experimental measurements (performed by Righi, 2003).

In Fig. 4, an incoming wind velocity $U = 11.69$ m/s is considered. The damped motion is qualitatively well reproduced. The energy exchange occurring during the motion between the two vibration modes is represented. Oscillation frequencies are modified by the action of self-excited forces, being the simulated vertical and torsional frequencies, respectively, $f_y = 5.98$ Hz and $f_\alpha = 7.81$ Hz, with a relative error of 4% and 0.8%, by comparison with experimental measurements.

In Fig. 5, wind velocity is $U = 15.54$ m/s. Coupling of vertical and torsional frequencies occurs, both in experimental tests and numerical simulations, at an intermediate flutter frequency between natural ones. This phenomenon is referred to as coupled flutter.

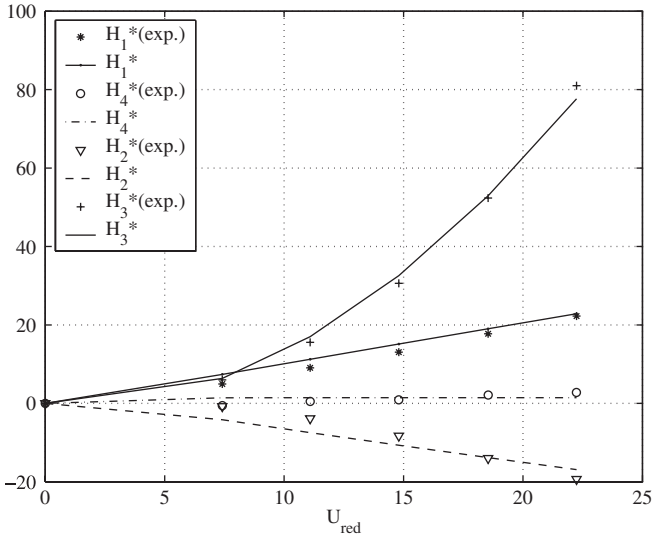

Fig. 2. Approximation of experimental derivatives H_i^* ($i = 1,\ldots,4$) via indicial functions ($B/D = 12.5$).

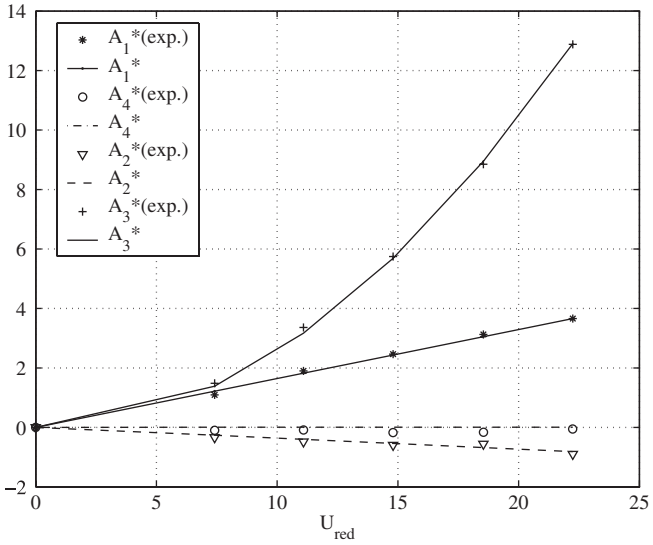

Fig. 3. Approximation of experimental derivatives A_i^* ($i = 1,\ldots,4$) via indicial functions ($B/D = 12.5$).

Table 2
Indicial functions—rectangular section $B/D = 12.5$

IF	a_i	b_i
Φ_{Ly}	0.9711	2.146
$\Phi_{L\alpha}$	1.0218	0.6636
Φ_{My}	0.2022	19.6084
$\Phi_{M\alpha}$	0.9541	2.0731

Table 3
Dynamic derivatives—rectangular section $B/D = 12.5$

C'_L	6.48
C'_M	1.04

By comparing experimental tests and numerical simulations, a very good accord in flutter frequency is observed. In fact, numerical flutter frequency is $f_{\text{crit}} = 7.32$ Hz and the relative distance from experimental results is of 0.7%. The amplitude of simulated displacements, thus, does not match exactly the experiments. In fact, wind tunnel records show the occurrence of frequency coupling but a still damped motion. This fact can be due to the occurrence of strong nonlinearities at flutter which may limit the amplitude of oscillations. Moreover, in experimental tests, rather than a unique wind velocity critical value, a range of wind velocities is identified producing frequency coupling. In this range, motion can be very sensible to perturbations. The value of wind velocity corresponding to frequency coupling is generally lower than wind velocity activating non-damped motion. This

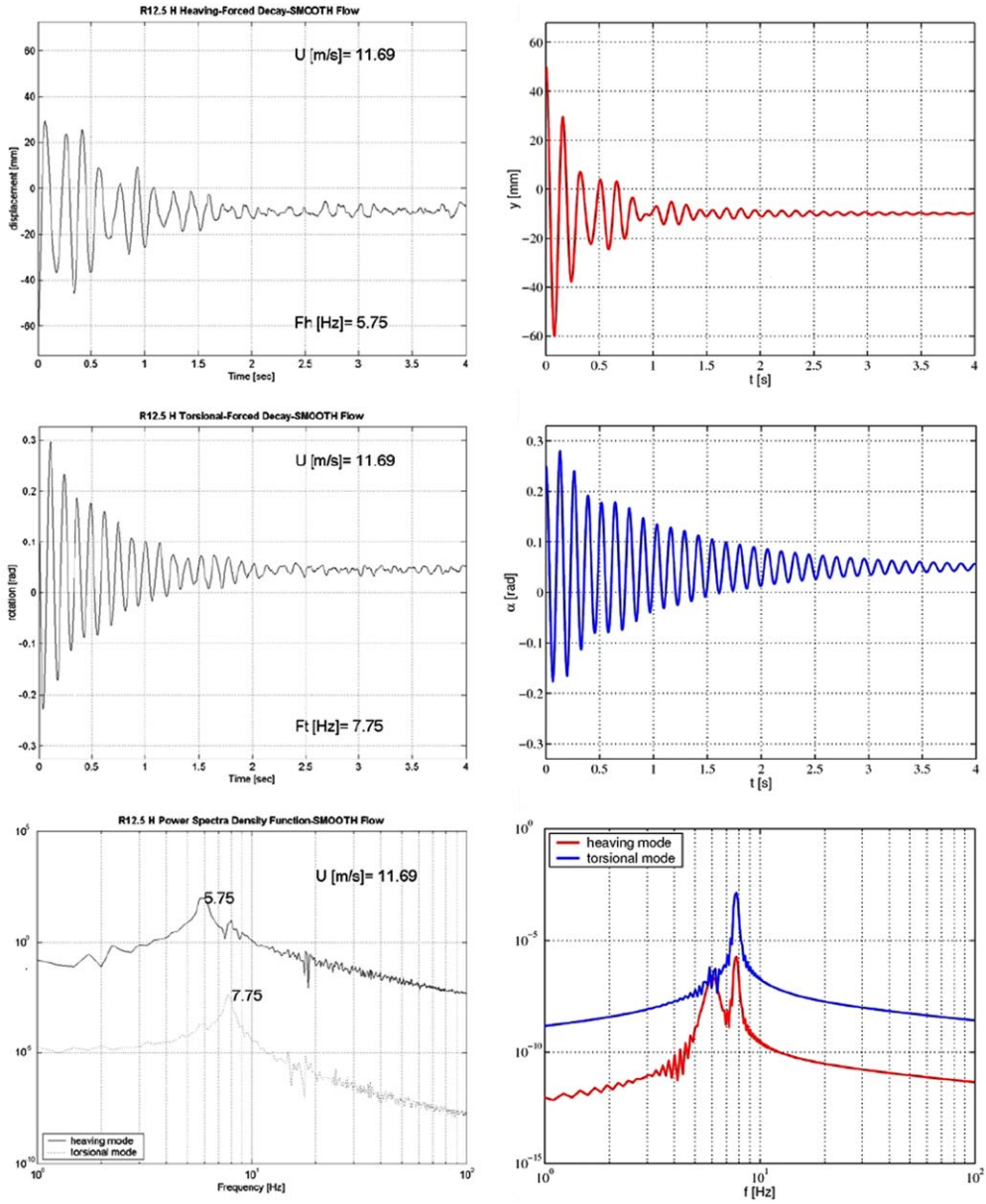

Fig. 4. Experimental test Righi (2003) (left) vs. numerical simulation (right)—$U = 11.69$ m/s.

circumstance is also pointed out in Righi (2003). Therefore, it can be assumed that the present model captures reasonably also flutter condition.

5.1.3. *Comparison of flutter analyses*

As a benchmark, an overview of results for coupled flutter is sketched in this paragraph (Table 4). In particular, following methods are compared: two eigenvalue analyses,

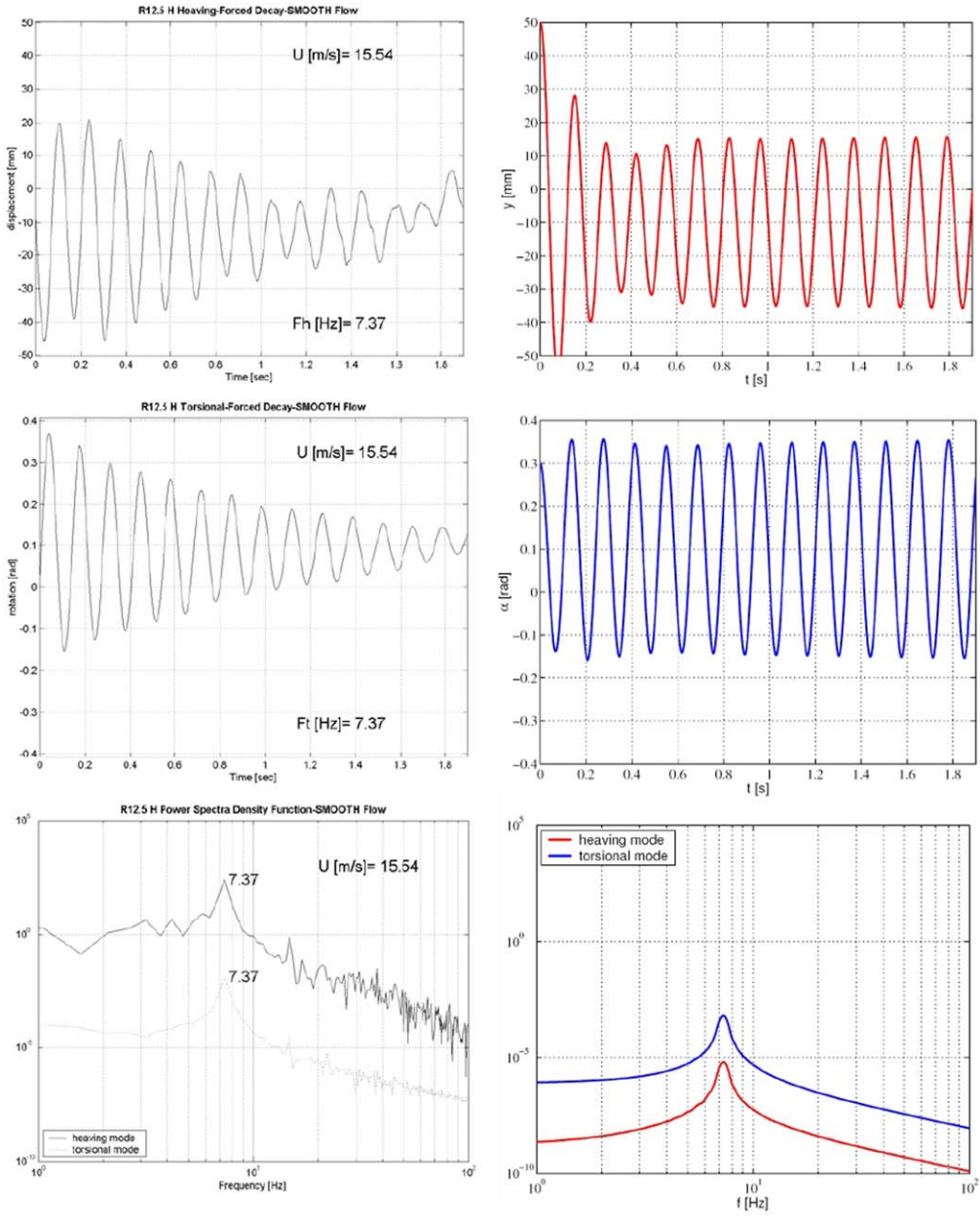

Fig. 5. Experimental test Righi (2003) (left) vs. numerical simulation (right)—$U = 15.54$ m/s.

performed with flutter derivatives expressed (a) by means of Theodorsen's function (as the theoretical flat plate), or (b) by means of experimental values; (c) time domain simulations, performed with the indicial model previously presented; (d) experiments results.

Flutter critical condition is assumed to correspond to coupling of natural frequencies with sinusoidal motion of the two DoFs.

In the eigenvalue analyses, critical speed calculated by means of theoretical derivatives is 12% higher than critical speed by means of experimental values, while a slight difference of 3% is observed on critical frequencies.

Results obtained with the indicial model are consistent, both for flutter frequency and velocity. In particular, the estimate of critical velocity is conservative. Calculated flutter threshold is 1% lower than the experimental value, while error on coupling frequencies is around 0.7%.

5.2. A bluff section

A rectangular section, with features given in Table 5, is analyzed. Dimensional ratio is $B/D = 5$.

Critical flutter velocity is calculated, by means of estimation of indicial coefficients and numerical simulations. Moreover, flutter velocity is identified by means of classical eigenvalue analysis and numerical simulations performed with indicial coefficients obtained form experimental data.

5.2.1. Identification of indicial function coefficients

Aeroelastic derivatives are taken from Matsumoto et al. (1996). Discrete data are interpolated by means of polynomial functions. A third-order polynomial approximation is selected for flutter derivatives, while a second-order approximation is chosen for A_2^*.

The simplest form with one exponential group is considered, at first, for all indicial functions. Identification results are plotted in Figs. 6 and 7.

Table 4
Comparison of flutter analyses—rectangular section $B/D = 12.5$

Flutter analysis method	U_{crit} (m/s)	f_{crit} (Hz)	$U_{red,crit}$
(a) Eigenvalues analysis (theor.)	19.90	6.84	7.76
(b) Eigenvalues analysis (exp.)	17.42	7.04	6.60
(c) Indicial function model	15.35	7.32	5.43
(d) Wind tunnel tests	15.54	7.37	5.75

Table 5
Geometrical and mechanical properties—rectangular section $B/D = 5$

L (m)	B (m)	ω_y (rad/s)	f_Y (Hz)	m (kg/m)	ζ_y (−)
0.920	0.10	24.50	3.90	3.157	0.0016
D (m)	B (m)	ω_α (rads^{-1})	f_α (Hz)	I (kg/m)	ζ_α (−)
0.04	0.20	48.38	7.70	0.010	0.0055

Aerodynamic coefficients are treated as unknown quantities, therefore estimated simultaneously with indicial coefficients.

Such an approximation well interpolates lift aeroelastic derivatives (Fig. 6), while a fair representation is obtained for moment aeroelastic derivatives (Fig. 7). In the other hand, if corresponding indicial functions are plotted, a slow growth to quasi-steady value can be observed. This fact corresponds to a certain significance of the unsteady effects, that is to a

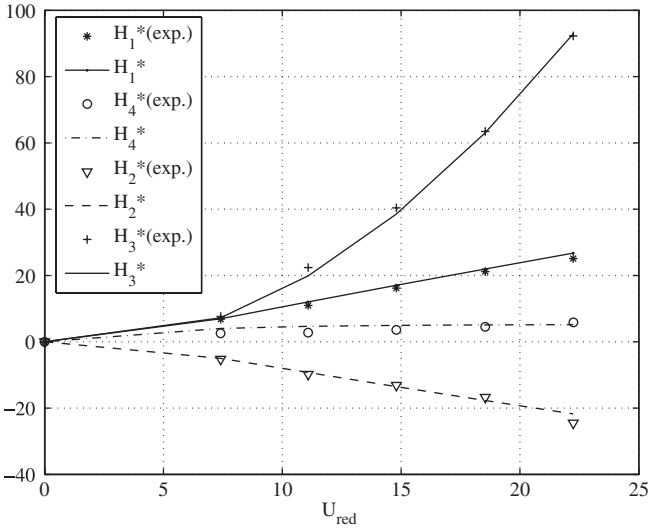

Fig. 6. Approximation of experimental derivatives H_i^* ($i = 1,\ldots,4$) via indicial functions ($B/D = 5$).

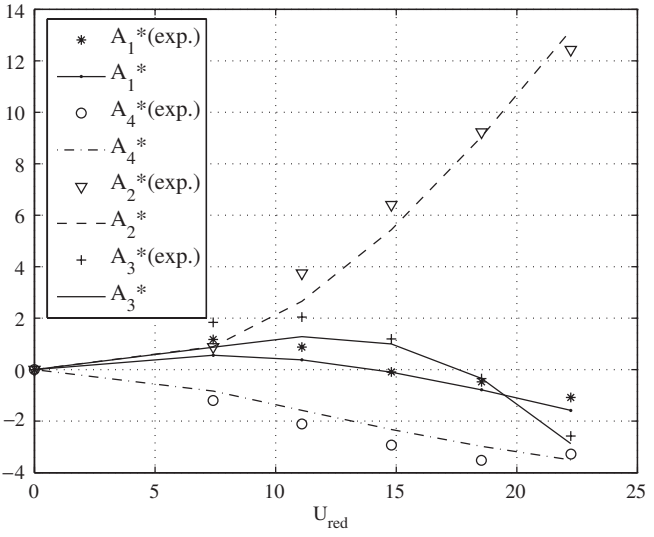

Fig. 7. Approximation of experimental derivatives A_i^* ($i = 1,\ldots,4$) via indicial functions ($B/D = 5$).

long memory effect on self-excited forces. Parameters characterizing indicial functions and dynamic derivatives are, respectively, in Tables 6 and 7.

Therefore, a deeper analysis is performed, assigning two exponential groups to the indicial approximation for moment derivatives, which are the most significant for the 'bluff' sections. A better approximation of moment aeroelastic derivatives is obtained, especially for A_2^* (Fig. 8). Parameters characterizing indicial functions and dynamic derivatives are, respectively, in Tables 8 and 9.

Comparison of corresponding indicial functions is shown in Fig. 9.

In the following, numerical simulations are compared for the two approximations.

Table 6
Indicial functions–Rectangular section $B/D = 5$ (one exponential group for H_i^* and A_i^*)

IF	a_i	b_i
Φ_{Ly}	1.0147	0.7437
$\Phi_{L\alpha}$	0.9589	0.5770
Φ_{My}	1.6047	0.1723
$\Phi_{M\alpha}$	1.6732	0.1445

Table 7
Dynamic derivatives—rectangular section $B/D = 5$ (one exponential group for H_i^* and A_i^*)

C'_L	7.84
C'_M	−1.26

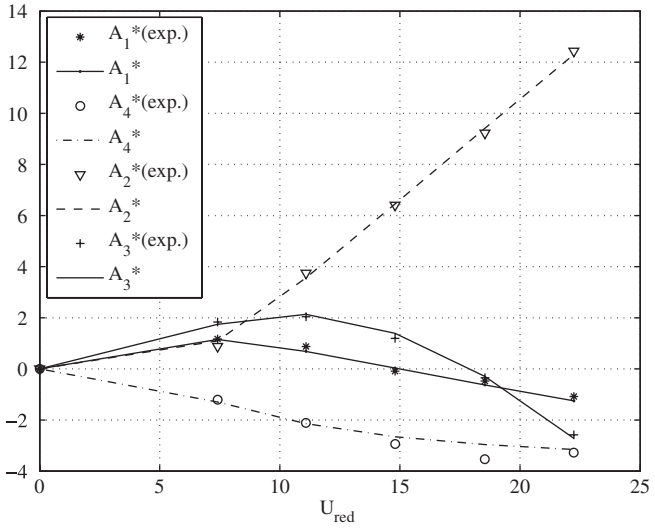

Fig. 8. Approximation of experimental derivatives A_i^* ($i = 1,\ldots,4$) via indicial functions ($B/D = 5$) (2 exponential groups).

5.2.2. Numerical simulations under wind loading

Numerical simulations show that the flutter phenomenon is driven, in this 'bluff' case, by twisting moment, being a typical case of *single-mode* flutter. It is pointed out the relevant significance of the approximation used for indicial functions. In fact, an insufficient approximation of aeroelastic derivatives influences the critical flutter condition and the overall behavior in pre-critical and post-critical range.

As observed in Fig. 10, at the incoming wind velocity $U = 7.20\,\text{m/s}$, torsional flutter is obtained for the section aerodynamically characterized by two exponential groups (right), while the other section (left) has a strongly diverging motion, having a lower flutter velocity. The vertical displacement, as observed in Fig. 11, has a relatively independent behavior from the torsional DoF, which drives the instability. Torsional frequency is not influenced at all by the vertical frequency (Fig. 12).

Table 8
Indicial functions—rectangular section $B/D = 5$ (one exponential group for H_i^* and two exponential groups for A_i^*)

IF	a_i	b_i	a_i	b_i
Φ_{Ly}	1.0147	0.7437	—	—
$\Phi_{L\alpha}$	0.9589	0.5770	—	—
Φ_{My}	4.5639	0.3838	−3.4781	1.7768
$\Phi_{M\alpha}$	6.6924	0.3688	−5.6613	0.8585

Table 9
Dynamic derivatives—rectangular section $B/D = 5$ (one exponential group for H_i^* and two exponential groups for A_i^*)

C'_L	7.84
C'_M	−0.74

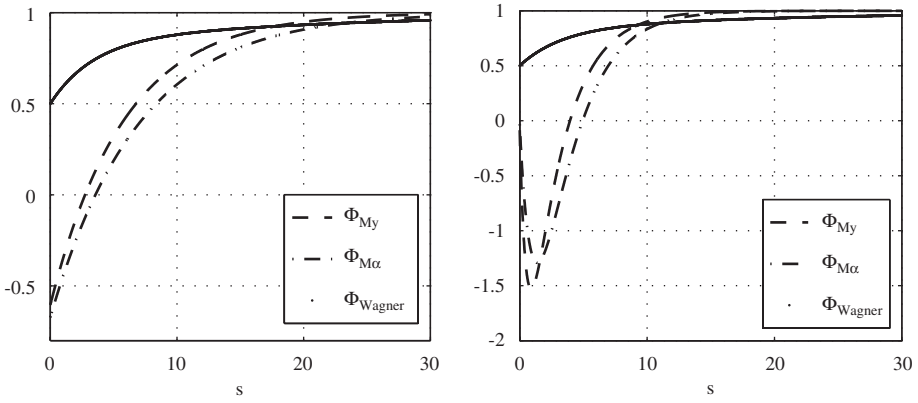

Fig. 9. Indicial functions $\Phi_{Mk}(s)$ obtained with one (left) and two (right) exponential groups and compared with Wagner's function.

5.2.3. Comparison of flutter analyses

An overview of results obtained for critical condition of single-mode flutter is resumed in Table 10. Critical wind velocity U_{crit} and frequency f_{crit} are calculated with different methods and compared with wind tunnel results obtained by Righi (2003). In particular, following methods are compared: two eigenvalue analyses, performed with flutter derivatives expressed (a) by means of Theodorsen's function (as the theoretical flat plate), or (b) by means of experimental values; time-domain simulations, performed with the indicial model and approximations of moment aeroelastic derivatives with (c) one or (d) two exponential groups; (e) experimental tests.

Flutter critical condition is assumed to correspond to sinusoidal motion of torsional DoFs.

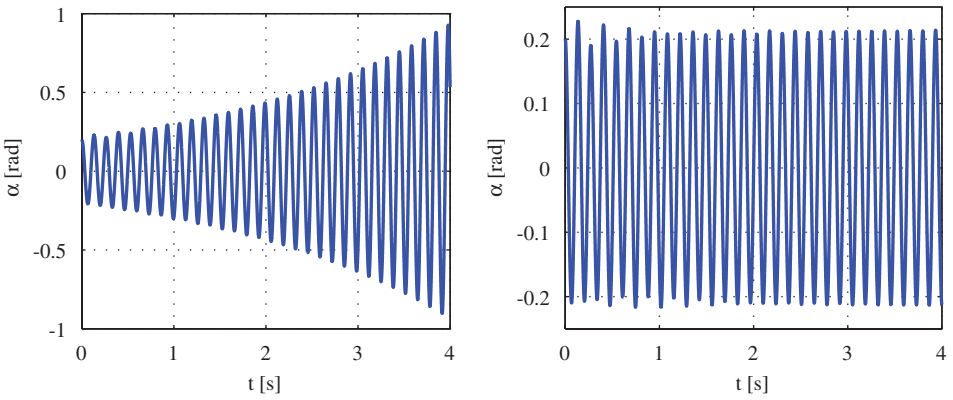

Fig. 10. Motion histories for torsional displacements with indicial functions characterized by one (left) and two (right) exponential groups—$U = 7.20$ m/s.

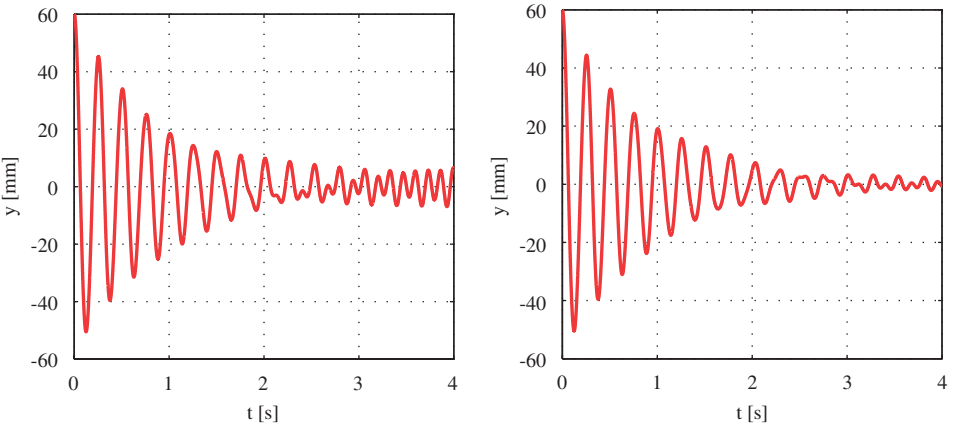

Fig. 11. Motion histories for vertical displacements with indicial functions characterized by one (left) and two (right) exponential groups—$U = 7.20$ m/s.

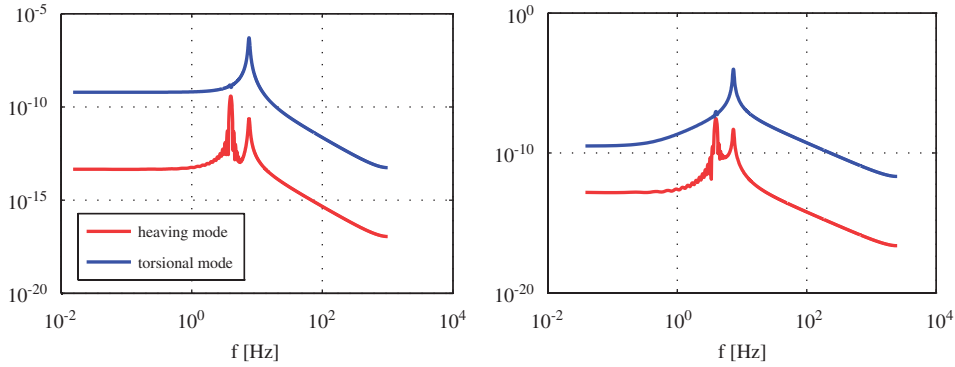

Fig. 12. PSD functions with indicial functions characterized by one (left) and two (right) exponential groups—$U = 7.20$ m/s.

Table 10
Comparison of flutter analyses—rectangular section $B/D = 5$

Flutter analysis method	U_{crit} (m/s)	f_{crit} (Hz)	$U_{red,crit}$
(a) Eigenvalues analysis (theor.)	20.32	5.19	19.59
(b) Eigenvalues analysis (exp.)	6.65	7.18	4.63
(c) Indicial function model (1)	5.35	7.59	4.06
(d) Indicial function model (2)	7.20	7.36	5.30
(e) Wind tunnel tests	6.90	7.34	5.06

In the eigenvalue analyses, critical speed calculated by means of theoretical derivatives is 67% higher than critical speed by means of experimental values, while a slighter difference of 38% is observed on critical frequencies. As expected, theoretical critical velocity is strongly overestimated. In fact, Theodorsen's function is able to capture sectional dynamics as much as the shape of the section is similar to the flat plate. Such a bluff body as a rectangular section with $B/D = 5$ has a totally different behavior. Better results are obtained by the eigenvalues analysis, if experimental flutter derivatives are considered.

Results obtained with the indicial model are consistent, but only in the case of indicial functions Φ_{Mk} characterized by two exponential groups. In fact, difference with experimental results, in this case, are equal to 4.3% for critical velocity and 0.3% for critical frequency, while in the case of moment aeroelastic derivatives approximated by one exponential group, differences are, respectively, 22% for critical velocity and 3.4% for critical frequency.

The energy due to self-excited moment excites also the vertical motion, as shown in Fig. 12 (left).

6. Conclusions

In this paper, an extensive analysis of indicial functions has been carried out, investigating the definition of the load model, the extraction of the indicial coefficients for rectangular cylinders and the comparison with other tools to define critical flutter speed.

Significant comparisons with experimental tests have been conducted in the case of the streamlined section with $B/D = 12.5$. In such case, an approximation of indicial functions with only one exponential is sufficient to capture sectional behavior in all ranges.

In the case of bluff section $B/D = 5$, indicial functions require approximations with more than one exponential groups to characterize not only the critical threshold, but also the sub-critical response.

In any case, stability threshold and pre-critical behavior can be successfully captured by the indicial function model, with a correct modeling of unsteady effects due to the fading memory of the fluid field forces.

Acknowledgments

This work has been performed under the Coordination of the COST action C14 on 'Impact of wind & storm on city life and built environment' (2000–2004) grouping experts and researchers from 16 countries worldwide. The financial support of MIUR within the research project of national interest (PRIN 2003) is gratefully acknowledged.

References

Bisplinghoff, R.L., Ahley, H., Halfman, R.L., 1955. Aeroelasticity. Dover Publication, Inc., Mineola, New York.

Boonyapinyo, V., Miyata, T., Yamada, H., 1999. Advanced aerodynamic analysis of suspension bridges by state-space approach. J. Struct. Eng. 125, 1357–1366.

Borri, C., Höffer, R., 2000. Aeroelastic wind forces on flexible girders. Meccanica 35 (10), 1–15.

Borri, C., Costa, C., Zahlten, W., 2002. Non-stationary flow forces for the numerical simulation of aeroelastic instability of bridge decks. Comput. Struct. 80, 1071–1079.

Bucher, C.G., Lin, Y.K., 1989. Stochastic stability of bridges considering coupled modes. J. Wind Eng. Ind. Aerodyn. 91, 609–636.

Caracoglia, L., Jones, N.P., 2003. Time domain vs. frequency domain characterization of aeroelastic forces for bridge deck sections. J. Wind Eng. Ind. Aerodyn. 91, 371–402.

Caracoglia, L., Jones, N.P., 2003. A methodology for the experimental extraction of indicial functions for streamlined and bluff deck sections. J. Wind Eng. Ind. Aerodyn. 91, 609–636.

Chen, X., Matsumoto, M., Kareem, A., 2000. Time domain flutter and buffeting response, analysis of bridges. Eng. Mech. ASCE 126 (1), 7–16.

Dyrbye, E.H., Hansen, R., 1996. Wind Effects on Structures. Kluwer Academic Publishers, Dordrecht.

Fung, Y.C., 1969. An Introduction to the Theory of Aeroelasticity. Dover Publication Inc., Mineola, New York.

Jones, R.T., 1940. The unsteady lift on a wing of finite aspect ratio. NACA Technical Report 681.

Lazzari, M., Vitaliani, R.V., Saetta, A.V., 2004. Aeroelastic forces and dynamic response of long-span bridges. Int. J. Num. Methods Eng. 60 (6), 1011–1048.

Lin, Y.K., Ariaratnam, S.T., 1980. Stability of bridge motion in turbulent wind. J. Struct. Mech. 8 (1), 1–15.

Lin, Y.K., Li, Q.C., 1993. New stochastic theory for bridge stability in turbulent flow. J. Eng. Mech. 119 (1), 113–127.

Matsumoto, M., Kobayashi, Y., Shirato, H., 1996. The influence of aerodynamic derivatives on flutter. J. Wind Eng. Ind. Aerodyn. 60, 227–239.

Matsumoto, M., Taniwakib, Y., Shijoa, R., 2002. Frequency characteristics in various flutter instabilities of bridge girders. J. Wind Eng. Ind. Aerodyn. 90, 1973–1980.

Righi, M., 2003. Aeroelastic stability of long span suspended bridges: flutter mechanism on rectangular cylinders in smooth and turbulent flow, Ph.D. Thesis. Università di Firenze, Italy.

Roger, K.L., 1977. Airplane Math Modelling Methods for Active Control Design. AGARD-CP-8 Advisory Group for Aerospace and Development, Neuilly-sur-Seine, France.

Scanlan, R.H., Jones, N.P., 1990. A minimum design methodology for evaluating bridge flutter and buffeting response. J. Wind Eng. Ind. Aerodyn. 36 (2), 1341–1353.

Scanlan, R.H., Tomko, J.J., 1971. Airfoil and bridge deck flutter derivatives. J. Eng. Mech. ASCE 97, 1717–1737.

Scanlan, R.H., Béliveau, J., K. Budlong, S., 1974. Indicial aerodynamic functions for bridge decks. J. Eng. Mech. Div. 100-EM4, 657–670.

Simiu, E., Scanlan, R.H., 1986. Wind Effects on Structures. Wiley, New York.

Theodorsen, T., 1935. General theory of aerodynamic instability and the mechanism of flutter, NACA Technical Report Aeronautics Twentieth Annual Report of the National Advisory Committee for Aeronautics, vol. 4, pp. 413–433.

Wagner, H., 1925. Über die Entstehung des dynamischen Auftriebes von Tragflügeln, ZAMM 5, Aeronautics Twentieth Annual Report of the National Advisory Committee for Aeronautics, pp. 17–35.

Wilde, K., Fujino, Y., Masukawa, J., 1996. Time domain modeling of bridge deck flutter. J. Struct. Eng./ Earthquake Eng. 13, 93–104.

Zahlten, W., Salvatori, L., Borri, C., 2004. Indicial functions or flutter derivatives: an evaluation for time domain simulations. In: Proceedings of IN-VENTO 2004, 8 Convegno Nazionale di Ingegneria del Vento, Reggio Calabria, Italy, 21–23 June 2004.

Zhang, X., Brownjohn, J.M., Omenzetter, P., 2003. Time domain formulation of self-excited forces on bridge deck for wind tunnel experiment. J. Wind Eng. Ind. Aerodyn. 91, 723–736.